doi.org/10.54473/IJTRET.2024.8102

International Journal of Trendy Research in Engineering and Technology
Volume 8 Issue 1 February 2024
ISSN No.2582-0958

A REVIEW ON FABRICATION TYPES OF MICRO/NANO HIERARCHICAL STRUCTURES AND THEIR APPLICATIONS IN AEROSPACE ENGINEERING

Lijalem Gebrehiwet[1], Amanuel Tadesse[1], Yared Negussie[2]
[1] Associate Researchers, Ethiopian Space Science and Technology Institute, Addis Ababa, Ethiopia
[2] Associate Researcher Manufacturing Technology and Engineering Industry R& D Center, Addis Ababa, Ethiopia
E mail: lijalemgg2013@outlook.com, amanueltadesse100@gmail.com[2], yared222@yahoo.com

Received 28 Feb 2024 Received in revised form 05 March 2024 Accepted 06 March 2024

ABSTRACT

This review paper discusses various nano/microstructures and fabrication techniques. The nano/ microstructure materials like nano/micropatterned polymer and hierarchical structured surfaces employ different fabrication processes which is the main purpose of this review paper to identify the best technique for Aerospace applications.. The common nano/micro patterned polymer surfaces fabrication technique is by using soft lithography. Hierarchical structured surfaces fabrication techniques are by using soft lithography, self-assembly and by drag reduction from shark skin. They have a special and excellent surface functions namely hydrophobicity, structure color, drag reduction, anti-adhesion, color camouflages and other features. Super hydrophobic surfaces are used for various applications, such as solar panels, cutlery, roof tiles, fabrics, self-cleaning windows, windshields, buildings paints, external paints for ships and others. The main applications in aerospace are the airfoil design, self-cleaning window glasses or paints and anti-corrosion metal surfaces. The methods employed to arrive on our specific applications are description on nano/micro hierarchical structures, useful natural replicas for these strictures, identifying their surface functions and unique benefits as well as the recommended fabrication processes and applications. The best application we found is the riblet fabrication used in airplanes and airfoils geometries. These hierarchical structured surfaces are fabricated by drag reduction from shark skin.

Keyword: Micro/nano hierarchical structures; lithography; surface functions; shark skin morphology; lotus effect

I. INTRODUCTION

The concept of Nano/Micro hierarchical surface structure comes from the nature which has splendid natural surfaces which can't see with naked eyes but with magnified glasses and the secret of the surfaces are not just as we saw them such as superhydrophobic. At high and low contact angle hysteresis; the superhydrophobic surfaces exhibit a self-cleaning effect. This property also exhibits low drag for fluid flow. Lotus leaves have super hydrophobic and self-cleaning (lotus effect) due to the hierarchical roughness of their leaf surfaces [1]. The other natural surface is the shark skin which has superior drag reduction feature which is called as shark skin effect. The one with micro morphology and the other is mucus or hierarchical structure. Shark skin is composed of diamond-arranged placoid scales of which the shapes are like small riblets which form tiny grooves in the flow direction. Microstructures were fabricated using a precision tooling machine on a flat aluminum sheet. They use mono crystalline diamond needle of 35 μm tip diameter and concaved microball arrays [2]. These days various artificial roughness induced hydrophobic surfaces have been fabricated with hierarchical structures. There are different methods to be employed such as Nanolithography, Photolithography, Colloidal systems, and Electro deposition [1]. In some papers it is demonstrated a simple and effective method of producing polymer super hydrophobic surfaces replicated by hierarchical micro/nano mold inserts Water contact angle increased from 89.7° on the flat surface to greater than 150° on hierarchical polymer structures without additional coating as shown in the figure below [2]. In Figure 1 the x-axis shows the mold inserts of microstructures where as y-axis shows the mold temperature of nanostructures.

The wettability of the surfaces is evaluated regarding the static and dynamic behavior of droplets. The contact angle hysteresis (CAH) is determined by the difference between advancing CA and receding CA. Depending on the angle CA formed by water droplet, the surfaces can be a hydrophilic (θ=90°) and super hydrophobic (θ >150°) as shown in Fig 1 [3].

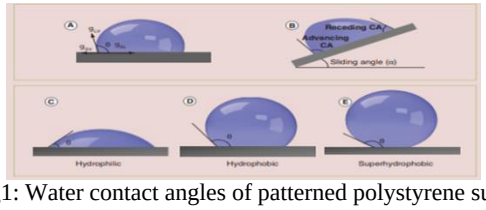

Fig1: Water contact angles of patterned polystyrene surfaces

"Lotus effect", i.e., self-cleaning and super hydrophobic property on lotus leaves as shown in the Figure 2 below. SEM images of the surface microstructure of a lotus leaf (images b and c), water droplet on the lotus leaf (image d), water droplet rolling on a lotus leaf (image e) and cassie wetting state between water droplet and the surface microstructure of a lotus leaf (images f) [4].

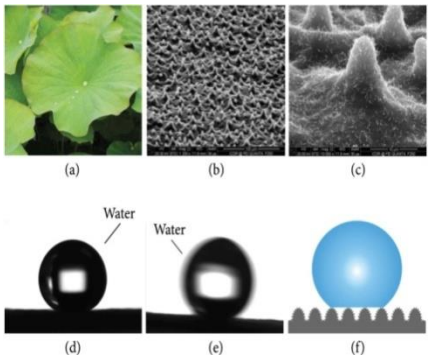

Fig 2: Super-hydrophobic property on lotus leaves and its effect

Water repellency is mainly caused by epicuticular wax crystalloids which cover the cuticular surface in a regular microrelief of about 1–5 μm in height [5]. Figure f shows schematic illustration of water-droplet cleaning on smooth and structured surfaces [6]. In some paper reviews five types of nature inspired drag reductions are available i.e. penguin-inspired microbubble, shark and dolphin skin-inspired, lotus leaf-inspired and others. The shark surface scale, groove, riblets surface etc. can be replicated by various materials namely polymer, silicon, metal, and so on. These natural profiles have a wide applications ranging from underwater vehicle to aircraft [7]. The relationship between the CD data and Re is described by the equation $CD=16.99Re^{0.47}$. Values of CD for the dolphins were compared with theoretical minimum drag coefficients. CD for dolphins ranged from 0.009 to 0.016 and all CD values were higher than the theoretical minimum values.

Dolphin skin inspired drag reduction can effectively control the laminar flow which ranges from 7–59%. This effect is widely used in ships, pipelines, aircraft, and e.t.c. [8]. Injecting micro-bubbles under high air pressure or by electrolysis process is used in penguin feather inspired microbubble drag reduction [9]. It mainly used in the military field and a maritime industry in both laminar and turbulent flow significant drag reduction efficiencies ranging from ~ 20% to ~ 80% have been achieved with this technique [10]. The superhydrophobic surfaces alter the symmetry, peak locations and magnitude of Reynolds stresses, [11]. Some researchers have obtained typically around 30%, up to 40% drag reductions on a macroscale (>1 m) object traveling at high speeds (5–10 knots) on open water [12].

The water repellency property for corrosion protection made them important for surface treatment. Super-hydrophobic surfaces have been widely applied on many metals and alloys of aluminum, magnesium, steel, titanium, zinc, copper and so on [13]. Superhydrophobic surface can be obtained for hydrophobicity, adhesion force, self-cleaning, and the performance of anticorrosion property. Superhydrophobic surface fabrication on Al substrate is shown in the Figure 3 below [14];

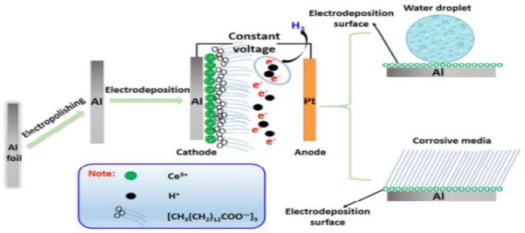

Fig 3. Schematic diagram for superhydrophobic surface fabrication on Al substrate.

Researchers use a simple operation, low-cost, low toxicity, and one-step method to fabricate a superhydrophobic surface with excellent self-cleaning properties, low adhesion force between water droplet and surface [14]. Corrosion resistance properties of super-hydrophobic surfaces have processes; formation of air layer within the valleys and minimizing the contact area as a barrier to hinders the corrosion of metal and alloy surface [15]. Most superhydrophobic surface has water contact angle larger than 150° and water sliding angle below 10°. Superhydrophobicity highly depends on both surface energy and micro-nano hierarchical structures [16]. In this review, we will be discussing various techniques for nanostructure fabrication such as nano/micro patterned polymer surfaces fabrication technique is by using soft lithography. The other is about hierarchical structured surfaces fabrication techniques for microstructures' fabrication using soft lithography, for fabrication of nanostructures by self-assembly and fabrication of drag reduction from shark skin. Finally the best method applied in aerospace applications will be recommended.

II. MICRO/NANO HIERARCHICAL STRUCTURES

An ideal hierarchical surface designation is shown below where the asperities rise high enough so that the droplet does not touch the valleys. They consist of circular pillars with diameter (D), height (H) and pitch (P) as shown in the Figure below. As an example for optimum nano asperities of a droplet radius in order of 1 mm or larger values of H, D and P, the values will be 30, 15 and 130 mm respectively [1] ;

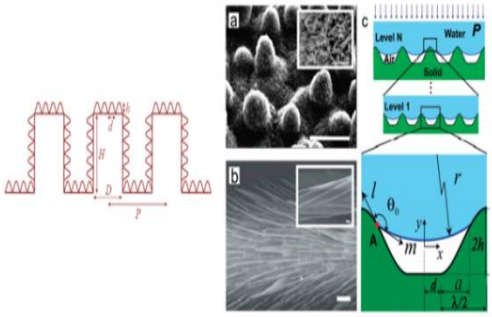

Fig 4. Hierarchical surface theoretical model and N-level hierarchical surface structure**.**

Nano-asperities can pin the liquid–air interface and thus prevent liquid from filling the valleys between asperities. Values with H and D of the order of 10 and 100 nm can be easily fabricated; [1] The main bottlenecks in the development of nanostructure hierarchical materials are; The current technologies are still far from being able to truly mimic nature and the second is related to the nature or sustainability of nanostructure hierarchical materials [17]. Naturally the lotus leaves exhibit two levels of hierarchy. The first level has characteristic dimension on the order of 100-500 nm and the second level on the order of 20 - 100 µm as shown in the Figure 4a below. Water strider's legs show a two-level hierarchy with the smallest structure size around 400 nm as shown in the Figure 4b [18].

III. MICRO AND NANO PATTERNED POLYMER SURFACES FABRICATION TECHNIQUES

According to different researchers, a nanosecond pulsed fibre laser with wavelength of 1064 nm was used to texture several different surfaces. This greatly facilitates the generation of surfaces having a high static friction coefficient. These surfaces have applications in large engines to reduce the tightening forces required for a joint [19]. Polytetrafluoroethylene (PTFE or Teflon) bulk material, PTFE films, and fluorinated silicone rubber/polyurethane coatings were investigated to understand their effects of chemical for surface roughness on ice adhesion and other categories [20].
Coatings that are intended to serve as anti-icing and de-icing agents must be able to reject water droplets and postpone the formation of ice. A NACA 0012 airfoil was coated and equipped with a thermal system along the stagnation line and piezoelectric actuators in the unheated aft region such ice protection system are designed and tested at Airbus, as seen in Figure 5 [20]

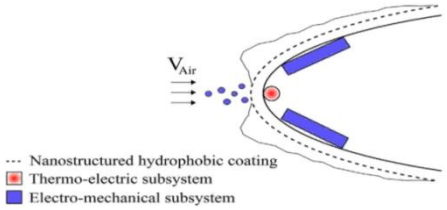

Fig 5. Illustration of the hybrid ice protection system

Researchers demonstrated laser surface modification of silicone rubber and showed that micro-nano structures led to an increase in the surface slope. The preparation of superhydrophobic silicone rubber has wide applications in self-cleaning, anti-icing, and anti-pollution [21]. This section provides a brief insight regarding strategies to fabricate various nano-micro-structural morphologies using various forms of nanomaterials such as nano-tubes, nano-particles, nano-fibers, nano-rods, nano-flakes, nano-wires and nano-sheets [22]. Microscale epidermal cells and nanoscale hair-like wax crystals are related to the surface structure properties of lotus leaves [23]. Recent advances in additive manufacturing (AM) like two-photon polymerization (TPP) enable the fabrication of more complex designs. Researchers presented a three-level hierarchical surface structure design that was influenced by numerous natural surfaces with cone, cuticle, and wrinkle patterns. The surface area/volume (SA/V) ratio for each level was modeled, and geometric designs were mathematically defined. A TPP technology was used for fabricating the proposed surface structures [24].
The water droplets roll down and gather debris as they fall off the leaf with the assistance of the nanoscale wax crystals. The scientific writers produced the illustration based on "Poole's idea illustration" [25]. Currently most of the researches on superhydrophobic materials are focused on the preparation technology. More growing researches are required on the wetting behavior of superhydrophobic materials [26].

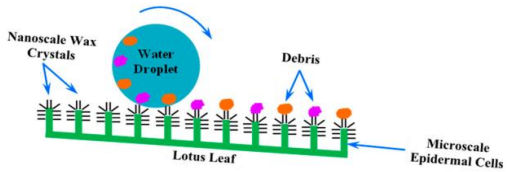

Fig 6. An easy-to-understand diagram showing how the water droplets gather the debris with a lotus effect

The superhydrophobic surfaces have recently attracted great focus as a result of their unique water repellency, self-cleaning, and anti-contamination properties. They have technical applications like self-cleaning window glasses, paints and for corrosion prevention [27].

Other applications stated by another researcher are Anti-icing, water and oil separation, flowing fluid drag reduction, anti-fouling paints for boats, anti bacterial adhesion, windshields and architecture coatings, and so on [28].

Fabrication using soft lithography:

Most commonly polymers used in nano technology nowadays are polymethyl methacrylate (PMMA) and polystyrene (PS). They are used to produce hydrophilic and hydrophobic surfaces. PMMA has hydrophilic groups with high surface energy where as PS has hydrophobic groups with low surface energy. Micro and nano patterned structures are manufactured using soft lithography.
To create micro-patterned structures, first cast a polydimethylsiloxane mold against a lotus leaf, and then heat it for a while. In order to generate a positive reproduction of the lotus leaf, the mold was finally placed on the PMMA and PS film [29].

IV. HIERARCHICAL STRUCTURED SURFACES FABRICATION TECHNIQUES

Hierarchical structures are composed of at least two levels of structuring in different length scales and fabricated surfaces with micro-patterned epoxy replicas, and lotus leaf microstructure. This uses wax tubules and platelets to produce a second level of structure [1]. The two steps of the fabrication process include the production of micro-structured surfaces by soft lithography and subsequent development of nanostructures. In the past decades, a great multitude of surface patterning methods have been created to fabricate various surface structures such as template synthesis, lithography, plasma treatment, phase separation, colloidal assembly, chemical vapor deposition, electrochemical deposition, layer-by-layer deposition, sol gel, electrospinning, and surface wrinkling [30]. SEM imaging was used to analyze the produced 3-level hierarchical microstructures in order to validate the design, as illustrated in Figure 7 below;

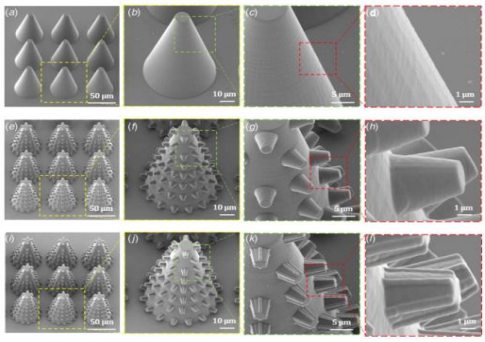

Fig 7. Printing surface structures using SEM pictures

However, suggested methods have some limitations such as expensive process, small area, or low durability. Thermoset or thermoplastic polymers and elastomer were considered for nano-hairy structures were used to enhance adhesion characteristics [24]. In order to resolve the above limitations, some researchers proposed the relatively easy and cost-effective method to fabricate micro-nano hierarchical structures for synthetic dry adhesives as shown below [31].

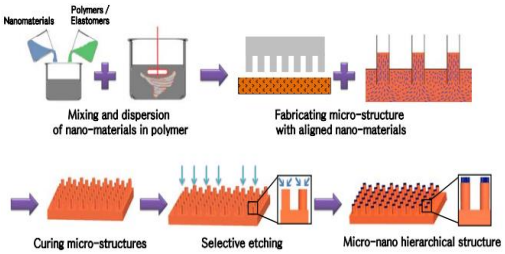

Fig 8. A novel technique for creating micro/nano hierarchical structures for artificial dry adhesives

Suggested method can have both flexibility of polymeric micro-structures, durability and superior adhesion of nano-structures simultaneously. Such method is cost-effective and used for mass production [32]. There are different ways of manufacturing layer-by-layer structures and described roughly as follows;

Microstructures' fabrication by soft lithography:

A two-step molding process was used to fabricate several structurally identical copies of the micro-patterned lotus leaves and Si surface. The molding process used is a fast, precise and low cost [33]. The method is used to mould a micro-structure. The Si surface is a pillar of 14 mm diameter, 30 mm height and 23 mm pitch fabricated by photolithography. The epicuticular wax tubules were removed in sections of around 6 cm^2 prior to the lotus leaf replicating.
The upper surface of the leaves is coated with fast-setting adhesive, which is then gently pressed onto the leaf. After hardening, the glue with the embedded waxes was removed from the leaf. The replication is a two-step molding process, in which first a negative replica of a template is generated and then a positive replica which is stated by different researchers [1].
A polyvinylsiloxane known as a dental wax. It is applied on the surface and pressed down with a glass plate immediately. After complete hardening of the molding mass, the negative mould and the silicon master surface will be separated. After 30 min, the negative replicas are filled with a liquid epoxy resin then after the specimens were immediately transferred to a vacuum chamber. The positive and negative replica will be separated after hardening at room temperature (22^0C for 24 hours) [34].

Some researchers created a stable, superhydrophobic surface using the nanoscale.
On the surface of the nanotubes, a small layer of conformal hydrophobic poly tetrafluoroethylene holds the forest of vertically aligned carbon nanotubes together [35]. TiO2 hierarchical structures along with sol gel based nano imprint lithography and hydrothermal growth fabrication process are shown below [36].

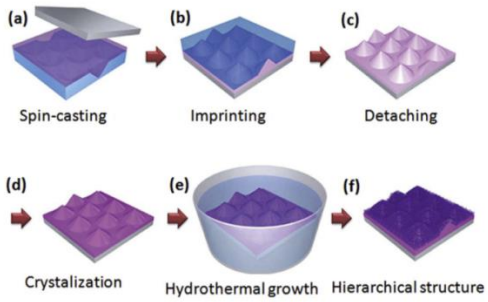

Fig 9. Schematic illustration of TiO2 hierarchical structures fabrication process

Lotus-leaf-like ZnO structures fabrication process are shown in the following steps;

- PDMS replication of fresh lotus leaf
- Replicated PDMS mold
- Soft imprint on ZnO sol film
- Imprinted ZnO sol–gel film
- Crystallized ZnO film after calcination
- Lotus-leaf-like ZnO micro-/nanostructures after hydrothermal reaction

Fabrication of nanostructures by self-assembly:

Nanostructure can be formed by self-assembly of synthetic and plant waxes deposits. Alkane n-hexatriacontane (C36H74) has been used for the development of platelet nanostructures. A thermal evaporation system is used for a homogeneous deposition of the waxes and alkane. Specimens of smooth surfaces or flat silicon replicas of micro-structured replicas were placed inside a vacuum chamber for heating [1]. The thermal evaporation system for self-assembly of a wax is shown below [37].

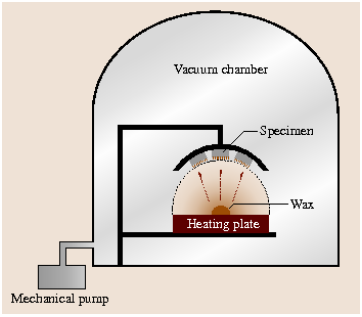

Fig 10. Schematic for thermal evaporation system

A wax nanostructure was created by using the alkane n-hexatriacontane (CH3 (CH2)34CH3) (98% purity, obtained from Sigma-Aldrich, Germany). This substance is capable of self-assembly. The behavior of wax crystals was observed using scanning electron microscopy [38].

Fabrication of drag reduction from shark skin:

Drag reduction lowering the resistance force between liquid and solid surfaces has long attracted wide attentions because of its intimate links with daily life and industrial processes. Various underwater creatures have been researched for morphological features possibly associated with drag-due-to-lift reduction [39]. Experimental evidence of the separation control capability of real shark skin through water tunnel testing was undertaken. A short fin mako *Isurus oxyrinchus* known for its outstanding speed and agility, they tested a pectoral fin and flank skin from the sample. They attached it to a NACA 4412 hydrofoil to observe separation control. The skin of a shark is covered with tiny placoid scales which are known as dermal denticles and embedded in the deeper collagenous layer of the skin. In Figure 11a_2, the size of placoid scales range from 0.2 mm to 0.5 mm. There are also some very fine and regularly spaced longitudinal grooves (width ~ 100 μm) [40].

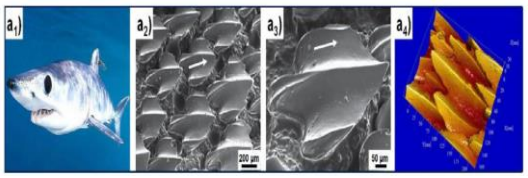

Fig 11. Shark skin tiny placoid scales

The micellar system has strong viscoelasticity, shear-thinning characteristics, and network structure. For underwater moving objects like submarines and torpedoes, the friction force can be up to ~ 80% of total resistance [41]. The research analyzes the simplest estimations of fish drag and power requirements during quasisteady motion. To reach high underwater velocity, the best swimmers need to have a low drag coefficient.

$$C_V = \frac{2X}{\rho U_\infty^2 V^{2/3}}$$

Where V volume of body moving at constant speed U_∞ in a fluid density of ρ and exhibits low drag X. A body moving at the same velocity in the water experiences drag that is around 800 times greater than that of a body moving in the [42]. The characteristic lengths were determined by the shapes of the fabricated objects for lotus-leaves-inspired super-hydrophobic and Nepenthes-pitcher-inspired slippery drag reduction, [43].

International Journal of Trendy Research in Engineering and Technology
Volume 8 Issue 1 February 2024
ISSN No.2582-0958

Because of its protrusion into the flow channel, the riblets profile increases surface area, which increases drag. The riblets should lift and pin the vortices and promote anisotropic flow around the surface in order to maximize drag reduction.

Sawtooth riblet airfoil experimentation table is shown in below [44]. We can fabricate riblets with a variety of polymers and metals using various fabrication and assembly processes. The actual process depends on many factors, such as costs, geometry, configuration, durability, precision, accuracy, base material, experimental set-up, chemical compatibility and sample set size.

Table: 1. Sawtooth riblet airfoil experimentation table

Reynolds number	Airfoil cross section description	Airfoil type	Sawtooth riblet size with h=s (μm)	Riblets applied to longitudinal location /chord length	Trip applied to longitudinal location /chord length	Angle of attack	Max drag reduction	Reference
17,000	Symmetrical	NACA 0012	180	0-100%	n/a	0°	4.3%	Han et al. (2003)
250,000	Symmetrical	NACA 0012	23, 76, 152	10-100%	n/a	0°	13.3%	Caram and Ahmed (1991)
530,000 - 790,000	Thin	LC 100D	76, 152	20-95%	2.5%	0°	2.7%	Coustols (1989)
750,000	Thin	GAW-2	114	12-96%	10%	0-6°	6%	Sundaram et al. (1999)
1,000,000	Symmetrical	NACA 0012	76, 152	12-96%	10%	0-6°	13%	Sundaram et al. (1996)
1,000,000	Thin	GAW-2	76	12-96%	10%	0-12°	10%	Subaschandar at al. (1999)
1,000,000	Thin	NACA 0012	76	12-96%	10%	0-12°	14%	Subaschandar at al. (1999)
1,000,000	Thick	NREL S807	114	5-100%	5%	0°	5%	Wetzel and Farokhi (1996)
1,000,000 - 1,850,000	Thick	DU 96-W-180	44, 62, 100, 152	40-100%	n/a	0°	5%	Sareen et al. (2011)
3,000,000	Thick	ADA-S1	18	15-100%	6%	-0.5-1°	10%	Viswanath and Mukund (1995)
3,300,000	Thin	CAST 7	17, 23, 33, 51	15-100%	n/a	0°	3.3%	Coustols and Schmitt (1990)
2,000,000 - 6,000,000	Symmetrical	NACA 0012	44, 100, 152	0-100%	5%	0°	7%	Present work
4,900,000 - 22,300,000	n/a	Conical nose with cylindrical body	33, 51, 76	87% coverage	n/a	0°	4%	Coustols and Cousteix (1994)

Feasible riblet fabrication techniques are; Metal shims, Machined acrylic, Embossed polymer, Grinding & rolling, Photolithography, Machined aluminium, Extruded polymer, Wet & dry etching and Soft lithography [44].

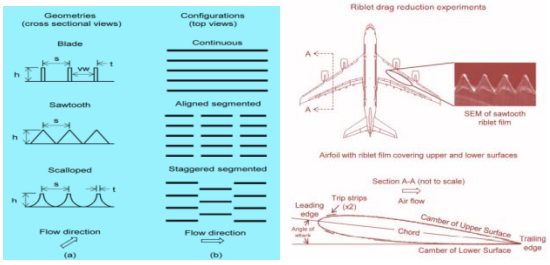

Fig 12. Typical shark skin experimentations of riblet geometries on airplanes and airfoils.

Figure 12 displays experimentally evaluated riblet geometries and arrangements inspired by shark skin. [44]. Researchers varied the riblet placement and size for each of the three Reynolds numbers to evaluate the riblet film. Every arrangement was put to the test across the whole low drag spectrum. The figure below illustrates laminar separation, reattachment, and riblet film sites on the DU 96-W-180 airfoils at angles of attack close to the upper corner of the drag polar (symbols refer to x/c locations, not the airfoil surface normal) [45];

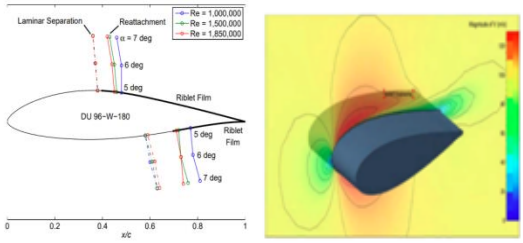

Fig 13. The locations of the reattachment and laminar separation points Airfoils DU 96-W-180

Figure 13 shows the velocity contour on both the baseline (no riblets) and with riblets. There is a small variation in the velocity contour on the upper surface. With riblets present, the separation region close to the trailing edge has somewhat decreased in size at zero angle of attack [46]. We compared various fabrication approaches of micro structure, and finally found that micro-molding and micro-embossing method is feasible to fabricate complicated morphology. The replication accuracy of shark skin can reach to 90% [1].

Table 1: Micro-molding and Micro embossing methods

Micro - molding	Micro - embossing
Template fixing (Shark skin)	Substrate heating (Shark skin)
PMMA tamping	Stacking and pressing
Flexibility remolding (replication mold)	Flexibility remolding (Replication mold)
Mold replication (Bio-mimetic skin)	Mold replication (bio-mimetic skin) Transverse and longitudinal views)

Shark skin also has excellent anti bio-fouling and can decrease microorganism fouling 70%. Shark constantly secrete mucus as swimming to keep higher drag reduction. To avoid waste of drag reduction agent, it is inevitable to graft drag reduction agent to substrate by chemical bonding for long-acting. The following methods can be used to bioreplicate shark skin's artificial drag reduction [44]. Taking PAM as drag reduction agent and the substrate material is water-based epoxy resin. Chemical graft reacts to form copolymer and the other fabrication approach is flexible micro-roll forming process. This has large area and simple manufacturing process. It has micro rolling process with micro grooves.

V. CONCLUSION

By replicating a micro-patterned silicon surface, the microstructure of a lotus leaf, and the self-assembly of wax platelets and lotus tubules, surfaces with micro, nano, and hierarchical structures can be created. It is flexible to fabricate a range of hierarchical structures using this two-step procedure. It is investigated how air pocket generation, adhesive force, static contact angle, contact angle hysteresis, tilt angle, and self-cleaning efficiency are affected by micro, nano, and hierarchical structures. It was demonstrated that adding roughness to the surfaces of micro/nano hierarchical structures enhanced their hydrophobicity. The adaptable and affordable method shows that hierarchical surfaces can be created in the lab for additional research into the characteristics of materials with hierarchical structures. Its self-cleaning effect made it suitable for corrosion resistance and surface treatment. From the various hierarchical structured surface fabrication techniques, fabrication of drag reduction from shark skin has a wide application to get shark skin inspired artificial riblets used in airplanes and airfoils geometries. According to different research reviews, airfoil with riblet films covering upper and lower surfaces of aircraft wing has higher drag reduction and smooth flow streams. Therefore shark skin inspired riblet geometries and configurations made it suitable in drag reduction for flying vehicles' designs.

REFERENCES

[1]. B. Bhushan, Y. Jung and K. Koch. 'Micro, nano and hierarchical structures for super hydrophobicity, self cleaning & low adhesion', Phil. Trans. R. Soc. A 367(2009) 1631-1672. doi:10.1098/rsta.2009.0014.

[2]. Ito et al. 'Micro and nano hierarchical structures on polymer surfaces for application to superhydrophobic properties'. IWMF 9th international workshop on micro-factories October 5-8, 2014, Honolulu, U.S.A.

[3]. Ana Catarina Lima, João. 'Micro/nano-structured super hydrophobic surfaces in the biomedical field, Basic concepts and biomimetic approach (Part I) Review', Nanomedicine (Lond.) 10(2015)103–119. Doi:10.2217/nnm.14.174.

[4]. Yong, J., Yang, Q., Hou, X., & Chen,'Nature-Inspired Superwettability Achieved by Femtosecond Lasers', *Ultrafast Science*, 2022(2023), Article ID 9895418, 51 pages. DOI: 10.34133/2022/9895418.

[5]. Barthlott, W., & Neinhuis, C. 'Purity of the sacred lotus, or escape from contamination in biological surfaces', *Planta*, 202(1997) 1-8. DOI: 10.1007/s004250050096.

[6]. Yu, C., Sasic, S., Liu, K., Salameh, S., Ras, R. H. A., & van Ommen, J. R. 'Nature-Inspired self-cleaning surfaces: Mechanisms, modelling, and manufacturing, *Chemical Engineering Research and Design*, 155(2020) 48-65. DOI: 10.1016/j.cherd.2019.11.038.

[7]. Yu, C., Liu, M., Zhang, C., Yan, H., Zhang, M., Wu, Q., Liu, M., & Jiang, L. (2020). 'Bio-inspired Drag Reduction: from Nature Organisms to Artificial Functional Surfaces', *Giant*, doi: 10.1016/j.giant.2020.100017.

[8]. Fish, F. E., Legac, P., Williams, T. M., & Wei, T. . 'Measurement of hydrodynamic force generation by swimming dolphins using bubble DPIV', *Journal of Experimental Biology*, 217 (2014), 252-260. DOI: 10.1242/jeb.087924.

[9]. Hassanalian, M. et al. 'Aquatic animal colors and skin temperature: Biology's selection for reducing oceanic dolphin's skin friction drag', *Journal of Thermal Biology*, 84(2019) 292-310. DOI: 10.1016/j.jtherbio.2019.07.018.

[10]. Elbing, B. R. et al. 'Bubble-induced skin-friction drag reduction and the abrupt transition to air-layer drag reduction', *Journal of Fluid Mechanics*.612(2008)201-236.
DOI: 10.1017/S0022112008003029.

[11]. Grabowski, A., Yu, N., Kerezyte, G., Lee, J. W., Pfeifer, B., & Kim, C. J. 'Superhydrophobic Drag Reduction for Turbulent Flows in Open Water', *Physical Review Applied*, 13(2020), 034056.
DOI: 10.1103/PhysRevApplied.13.034056

[12]. Xu, M., Grabowski, A., Yu, N., Kerezyte, G., Lee, J. W., Pfeifer, B. R., & Kim, C.-J. 'Superhydrophobic Drag Reduction for Turbulent Flows in Open Water', *Physical Review Applied*, 13(2020)034056.
DOI: 10.1103/PhysRevApplied.13.034056

[13]. Zhao, G., Xue, Y., Huang, Y., Ye, Y., Walsh, F. C., Chen, J., & Wang, S. 'One-Step Electrodeposition of a Self-Cleaning and Corrosion Resistant Ni/WS2 Superhydrophobic Surface', *RSC Advances*, 6(2016) 59104–59112. DOI: 10.1039/c6ra07899k

[14]. Zhang, B., Li, Y., & Hou, B. 'One-step electrodeposition fabrication of a superhydrophobic surface on an aluminum substrate with enhanced self-cleaning and anticorrosion properties', *RSC Advances*,

5(2015) 100000–100010. DOI: 10.1039/C5RA21525K

[15]. Wu, L.-K., Zhang, X.-F., & Hu, J.-M. 'Corrosion protection of mild steel by one-step electrodeposition of superhydrophobic silica film', *Corrosion Science*, 85(2014). 482–487. DOI: 10.1016/j.corsci.2014.04.026

[16]. Bi, P., Li, H., Zhao, G., Ran, M., Cao, L., Guo, H., & Xue, Y. 'Robust Super-Hydrophobic Coating Prepared by Electrochemical Surface Engineering for Corrosion Protection. *Coating's*, 9(2019) 452. DOI: 10.3390/coatings9070452

[17]. Martin-Martinez, F. J., Jin, K., López Barreiro, D., & Buehler, M. J. 'The Rise of Hierarchical Nanostructured Materials from Renewable Sources: Learning from Nature', *ACS Nano*, 12(2018)7425–7433. DOI: 10.1021/ACSNANO.8B04379

[18]. Su, Y., Ji, B., Zhang, K., Gao, H., Huang, Y., & Hwang, K. ' Nano to micro structural hierarchy is crucial for stable superhydrophobic and water-repellent surfaces', *Langmuir*, 26(2010), 4984–4989. DOI: 10.1021/la9036452

[19]. Dunn, A., Carstensen, J. V., Wlodarczyk, K. L., Hansen, E. B., Gabzdyl, J., Harrison, P. M., Shephard, J. D., & Hand, D. P. 'Nanosecond Laser Texturing for High Friction Applications', *Optics and Lasers in Engineering*, 62(2014) 9–16. DOI: 10.1016/j.optlaseng.2014.05.003

[20]. Xiao, H., Nick, T., Valérie, P.-B., Marc, B., Elmar, B., Philippe, V., & Lokman, B. 'A survey of icephobic coatings and their potential use in a hybrid coating/active ice protection system for aerospace applications', *Progress in Aerospace Sciences*, 105(2019) 74–97. ISSN: 0376-0421. DOI: 10.1016/j.paerosci.2018.12.001

[21]. Parvate, S., Dixit, P., & Chattopadhyay, S. (2020). Superhydrophobic Surfaces: Insights from Theory and Experiment. *The Journal of Physical Chemistry B*, 124, 1323−1360. DOI: 10.1021/acs.jpcb.9b08567

[22]. Kim, W., Kim, D., Park, S., Lee, D., Hyun, H., & Kim, J. .' Engineering lotus leaf-inspired micro- and nanostructures for the manipulation of functional engineering platforms', *Journal of Industrial and Engineering Chemistry*, 61(2018) 39–52. DOI: 10.1016/j.jiec.2017.11.045

[23]. Lichade, K. M., Jiang, Y., & Pan, Y. 'Hierarchical Nano/Micro-Structured Surfaces with High Surface Area/Volume Ratios', *Journal of Manufacturing Science and Engineering*, 143(2021), 081002. DOI: 10.1115/1.4049850

[24]. Collins, C. M., & Safiuddin, M. 'Lotus-Leaf-Inspired Biomimetic Coatings: Different Types, Key Properties, and Applications in Infrastructures', *Infrastructures*, 7(2022), 46. DOI: 10.3390/infrastructures7040046

[25]. Hao, P., Yao, Z., & Zhang, X, 'Study of dynamic hydrophobicity of micro-structured hydrophobic surfaces and lotus leaves', *Science China Physics, Mechanics & Astronomy*, 54(2011) 675–682. DOI: 10.1007/s11433-011-4269-1

[26]. Safiuddin, Md., Hossain, K., & Collins, C. M. (2018). 'Potential applications of self-cleansing nano lotus leaf biomimicked coating in different construction sectors', *Conference paper, CSCE, Building Tomorrow's Society*, MA61-1-MA61-9

[27]' Vazirinasab, E., Jafari, R., & Momen, G. ' 'Applications of Superhydrophobic Coatings as a Corrosion Barrier: A Review', *Surface and Coatings Technology*, 341(2018) 40–56. DOI: 10.1016/j.surfcoat.2017.11.045

[28]. Jung, Y. C., & Bhushan, B. ' Contact angle, adhesion, and friction properties of micro- and nano-patterned polymers for super hydrophobicity', Nanotechnology, 17(2006), 4970–4980. doi: 10.1088/0957-4484/17/19/033 .

[29]. Gur, H. –Y et al. 'Functional map of biological and biomimetic materials with hierarchical surface structures', RSC Advances, 5(82)(2015). DOI: 10.1039/C5RA09490A

[30]. Hwang, H. Y., & Han, S. H. (2018). 'Fabrication of Micro-nano Hierarchical Structures with Multiwall Carbon Nanotubes and Poly (Dimethylsiloxane)', Proceedings of the 18th European Conference on Composite Materials (ECCM18), *Athens, Greece.*

[31]. Kim, G. H., Ahn, T. C., & Hwang, H. Y. 'Adhesive Strength of Dry Adhesive Structures Depending on the Thickness of Metal Coating. Transactions of the Korean Society of Mechanical Engineers', Part A, *40(2016), 673-677.*

[32]. Koch, K., Dommisse, A., Barthlott, W., & Gorb, S. '*The use of plant waxes as templates for micro- and nano-patterning of surfaces. Acta Biomaterialia'*, 3(2007) 905–909. doi: 10.1016/j.actbio.2007.05.013.

[33]. Lau, K. K. S., Bico, J., Teo, K. B. K., Chhowalla,

M., Amaratunga, G. A. J., Milne, W. I., et al. ' *Superhydrophobic carbon nanotube forests*', *Nano Letters*, 3(2003) 1701–1705. doi: 10.1021/nl0348456.

[34]. Liu, H., Feng, L., Zhai, J., Jiang, L., & Zhu, D. '*Reversible wettability of a chemical vapor* deposition prepared ZnO film between superhydrophobicity and super hydrophilicity', *Langmuir*, 20(2004), 5659–5661. doi: 10.1021/la049776v.

[35]. Bhushan, B., Jung, Y.-C., & Nosonovsky, M. (2010). ' *Lotus effect: surfaces with roughness-induced super hydrophobicity, self-cleaning, and low adhesion*', In B. Bhushan (Ed.), *Springer Handbook of Nanotechnology* (pp. 1436–1524). Springer. doi: 10.1007/978-3-64202525-9_42.

[36]. Šprdlík, V., Kotradyová, V., & Tiňo, R. '*Superhydrophobic Coating of European Oak, European Larch, and Scots Pine Wood Surfaces*', *BioResources*, 12(2017), 3289-3302. doi: 10.15376/biores.12.2.3289-3302.

[37]. Bushnell, D. M., & Moore, K. J. ' *Drag reduction in nature. Annual Review of Fluid Mechanics'*, 23(1991), 65–79. doi: 10.1146/annurev.fl.23.010191.000433.

[38]. Lang, A. W., Bradshaw, M. T., Smith, J. A., Wheelus, J. N., Motta, P. J., Habegger, M. L., & Hueter, R. E. '*Movable shark scales act as a passive dynamic micro-roughness to control flow separation. Bioinspiration & Biomimetics'*, 9(2014), 036017. doi: 10.1088/1748-3182/9/3/036017.

[39]. Gu, Y., Yu, S., Mou, J., Wu, D., & Zheng, S. ' *Research progress on the collaborative drag reduction effect of polymers and surfactants*', *Materials*, 13(2020) 444. doi: 10.3390/ma13020444.

[40]. Nesteruk, I., Passoni, G., & Redaelli, A. ' *Shape of aquatic animals and their swimming efficiency*',*Journal of Marine Biology*, (2014), 1–9. doi: 10.1155/2014/470715.

[41]. Fox, R. W., & McDonald, A. T. (2011). '*Introduction to Fluid Mechanics'*, (11th ed.). New York: John Wiley & Sons.

[42]. Bixler, G. D., P.E., & M.S. (2013). '*Bioinspired Surface for Low Drag, Self-Cleaning and Antifouling: Shark Skin, Butterfly and Rice Leaf Effects'*. Project report, Ohio State University.

[43]. Sareen, A., Deters, R. W., Henry, S. P., & Selig, M. S. (2011). '*Drag reduction using riblet film applied to airfoils for wind turbines*', Paper # AIAA-2011-558, presented at the 49th AIAA Aerospace Sciences Meeting, Orlando, FL. AIAA.

[45]. Sidhu, B. S., Saad, M. R., Ku Ahmad, K. Z., & Che Idris, A. ' *Riblets for airfoil drag reduction in subsonic flow', ARPN Journal of Engineering and Applied Sciences*, 11(2016), 3289-3302. doi: 10.1819/6608.

[46]. Zhang, D., Li, Y., Han, X., Li, X., & Chen, H. .'*High-precision bio-replication of synthetic drag reduction shark skin', Chinese Science Bulletin, Bionic Engineering*, 56(2011) 938–944. doi: 10.1007/s11434-010-4163-7.